Chapter 6
POD Analysis on Losing Symmetry of Vortex Structure in the Flow Transition by Liutex Method

Pushpa Shrestha, Charles Nottage, and Chaoqun Liu

Abstract The proper orthogonal decomposition (POD) is a data decomposition method to investigate and analyze complex turbulent flow. The POD method offers the optimal low-dimensional approximation of a given data set. In our case, POD is used with Liutex vector as an input instead of velocity vector to extract the coherent structure of late boundary layer flow transition. Mathematically, the Liutex vector field is decomposed into a sum of basis functions (spatial modes) multiplied by time coefficients (Fourier-splitting method). A singular value decomposition (SVD) algorithm is used to perform the POD method. Our studies show that fluid motion can be modeled/reconstructed by a few leading modes as they contain a large portion of total rotational intensity. Trailing modes can be neglected as they do not contribute to the total rotational strength of the flow. From the reconstructed vortex structure in the flow transition, the loss of symmetry of vortex is investigated, and it is found that the asymmetry of vortex develops at the flow transition. In fact, our study shows that the antisymmetric of the vortex starts from the middle, and then the antisymmetric structure of the bottom part starts and spreads to the top level.

6.1 Introduction

The proper orthogonal decomposition (POD) method is a highly applied data analysis and modeling method in fluid mechanics. The POD method allows us to reconstruct a flow with the first few most energetic modes, keeping the data structure intact. Sometimes, the fluid motion is not easily visible in raw data; in this case, reconstructed POD modes can model the fluid motion accurately and efficiently. This method essentially offers an orthogonal basis to represent a given set of data where optimal low-dimensional approximations for the given data set are calculated [1, 2]. The bases are also known as POD modes. These POD modes best represent the data. The leading modes represent most of the rotational intensity of incompressible flow, whereas high-ordered POD modes represent very few portions of total rotational

P. Shrestha · C. Nottage · C. Liu (✉)
Department of Mathematics, The University of Texas at Arlington, Arlington, TX 76019, USA
e-mail: cliu@uta.edu

Y. Wang et al. (eds.), *Liutex and Third Generation of Vortex Identification*,
Springer Proceedings in Physics 288, https://doi.org/10.1007/978-981-19-8955-1_6

strength. We choose the Liutex vector as an input vector instead of a velocity vector [3]. Most POD analysis has been done with the velocity vector as an input. However, in this study, we use the Liutex vector as an input as Liutex represents the local rigid rotation part of fluid motion without shear and stretching/compression contamination [4]. The velocity modes are related to the kinetic energy content, whereas the Liutex mode represents the rotation intensity. Since the Liutex vector represents local rigid rotation of fluids without any shear or stretching contamination, the Liutex vector is applied instead of the velocity vector as an input for POD analysis.

A vortex is known as the rotational fluid movement. Over the past three decades, several vortex identification methods such as Q, Δ, λ_2, andλ_{ci} have been suggested and used in direct numerical simulation (DNS) data to analyze and visualize the vortex structure numerically in the transitional boundary layer [5–8]. These methods are based on scalar quantities and need a proper threshold to capture the vortex boundary. According to Liu et al. [9], vorticity-based methods are classified as the first generation (1G) of vortex identification methods, eigenvalue -based methods such as Q, Δ, λ_2, andλ_{ci} are regarded as the second generation (2G) of vortex identification methods, and the Liutex method [10, 11], Liutex-Core–Line method, and other Liutex-based methods [12, 13] are regarded as the third-generation (3G) of vortex identification methods. The third generation of vortex identification methods is considered the best among the prevalent methods as it can present accurate vortex boundaries along with the direction [14, 15]. Since then, the novel Liutex has been used abundantly in the literature by many fellow researchers and scientists [16–18].

The POD method is one of the most broadly applied modal decomposition and dimensionality reduction techniques to analyze vortex structure. There are two versions of the POD method. Initially, the POD method was proposed by Lumley [1] in 1967 to explore the turbulent flow. In 1987 Sirovich [2] introduced the other version of POD known as snapshot POD. Both versions of POD are equivalent to the singular value decomposition (SVD) method. So SVD method is used in this paper for POD analysis of late flow transition. In the POD method with Liutex input vector, the orthogonal modes are ranked according to their rotational intensity. The first mode contains the largest rotational intensity of the flow and gradually decreases as we go on to the next mode. Due to limited computer memory, POD modes with high intensity are used to optimize the computation. Many researchers have used the POD method to study the flow structure. POD was used in research [19, 20] to analyze the flow structures in various cases and scenarios. Dong et al. applied POD analysis on vortical structures in MVG wake by Liutex core line identification [21]. The POD method has also been applied to flow transition in the boundary layer. Gunes used the POD method to reconstruct a transitional boundary layer with and without control [19]. Yang et al. studied the POD analyses on vortex structure in the late transition [20].

In this paper, POD is applied to study and analyze the conversion of the symmetric vortex to asymmetry in the flow transition with a Liutex input vector to reconstruct the data. The modified Liutex-Omega vortex identification method is applied to DNS data to capture the vortex structure of flow transition with iso-surfaces of $\Omega_L = 0.52$ and $\varepsilon = 0.001(b-a)_{max}$. Due to the limited computer memory capacity, snapshot POD is used here.

6.2 Numerical Setup

First, a snapshot matrix A is taken from DNS data of the flat plate boundary layer with 100 snapshots in time between $t = 20.505T$ to $t = 21.00T$, where T is the period of Tollmein-Schlichting wave, to study orthogonal basis functions (POD modes) of the coherent vortex structures in the transitional flow. Then, we have chosen the proper subzone in the late boundary layer transition defined by the parameters given in Table 6.1 to study the POD of flow structure (Fig. 6.1).

The table gives the starting and ending points of index i, j, k along x, y and z directions.

The snapshot matrix A between the timesteps $t = 20.5T$ to $t = 21.0T$ is given by,

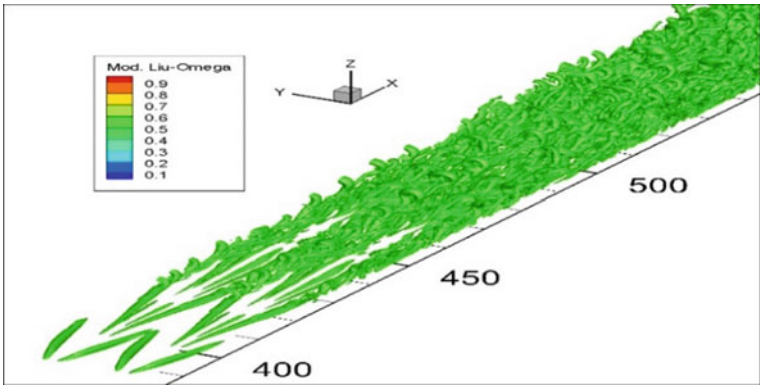

Fig. 6.1 Vortex structure of transitional boundary layer by modified Liutex-Omega method

Table 6.1 Parameters of subzone

Grid direction	Starting index	Ending index
i	500	580
j	1	128
k	1	200

$$\mathrm{A} = \begin{pmatrix} L_{x\,500,1,1}^{(j)} \\ \vdots \\ L_{x\,580,128,200}^{(j)} \\ L_{y\,500,1,1}^{(j)} \\ \vdots \\ L_{y\,580,128,200}^{(j)} \\ L_{z\,500,1,1}^{(j)} \\ \vdots \\ L_{z\,580,128,200}^{(j)} \end{pmatrix} \text{for} j = 1, \ldots, 100,$$

where ${L_x}^{(j)}$, ${L_y}^{(j)}$ and ${L_z}^{(j)}$ are Liutex vectors in x, y, z directions in the flow fields at several time steps $t = (20.50 + 0.005j)T$ where j is from 1 to 100.

6.3 Proper Orthogonal Decomposition (POD)

The POD modes, also known as the orthogonal basis, are ranked by fluctuating rotational intensity, where leading modes have the dominant rotational intensity, and trailing modes have weak or no rotational intensity.

Definition 6.1 POD modes are the orthogonal basis for the given data set. In fluid mechanics, they are a set of deterministic spatial functions received from the decomposition of the random vector field representing the turbulent fluid motion. Each of these functions, also known as POD modes, can capture some portion of the rotational strength of the flow.

Let $u(\mathrm{x}, \mathrm{y}, \mathrm{z}, \mathrm{t})$ denote the vector field in the flow with fluctuating velocity. Then,

$$u(\mathrm{x}, \mathrm{y}, \mathrm{z}, \mathrm{t}) = U(\mathrm{x}, \mathrm{y}, \mathrm{z}) - U'(\mathrm{x}, \mathrm{y}, \mathrm{z}), \tag{6.1}$$

where $U(\mathrm{x}, \mathrm{y}, \mathrm{z})$ is the velocity vector, and $U'(\mathrm{x}, \mathrm{y}, \mathrm{z})$ is the temporal mean velocity vector (assumed to be stationary). Then, the POD method decomposes the random vector field $u(\mathrm{x}, \mathrm{y}, \mathrm{z}, \mathrm{t})$ into a sum of orthogonal basis functions/POD modes $\Phi_k(x, y, z)$ multiplied by random time coefficients $\mathrm{a}_k(t)$, i.e.,

$$u(\mathrm{x}, \mathrm{y}, \mathrm{z}, \mathrm{t}) = \sum_{k=1}^{\infty} \mathrm{a}_k(t)\Phi_k(x, y, z) \tag{6.2}$$

Here, Φ_k is the matrix of eigenvectors of the covariance matrix $\frac{1}{m-1}U^T U$, where m is rows of U.

In matrix form, it can be written as:

$$A = \Phi Q \tag{6.3}$$

where the matrix Φ contains the spatial modes $\Phi_k(x, y, z)$ and Q contains the temporal coefficients $a_k(t)$.

6.4 POD Analysis Inflow Transition by Modified Liutex Omega Method

We have used SVD to perform the POD method, and the singular values are ordered in ascending order. Figure 6.2 shows the contribution of each mode to total fluid rotational intensity. The amount of the rotational intensity possessed by higher modes gradually decreases, and ultimately, they converge to zero.

The following figures represent the structure of the first six POD modes. The other modes have similar vortex structures, so we have not included them (Fig. 6.3).

Mode 1, also known as mean flow, has the dominant streamwise vortex stricture. Mode 2, 3, and 4 also have the streamwise vortex structure but are less intense than mode 1. Spanwise characteristic dominates the vortex structure in higher modes as higher modes show more fluctuation distributions of vortex structures. In other words, the streamwise vortex structure is dominant in the leading modes, whereas the spanwise characteristic is dominant in the trailing modes. This nature of POD modes can be seen through the interior vortex structure, shown in Fig. 6.4.

Since the leading modes with streamwise structures possess significantly higher rotational strength than the other trailing modes, the original vortex structures can be reconstructed by a few leading modes. So, we can model the original flow by reconstructing the data of the first few POD modes that have major contribution to

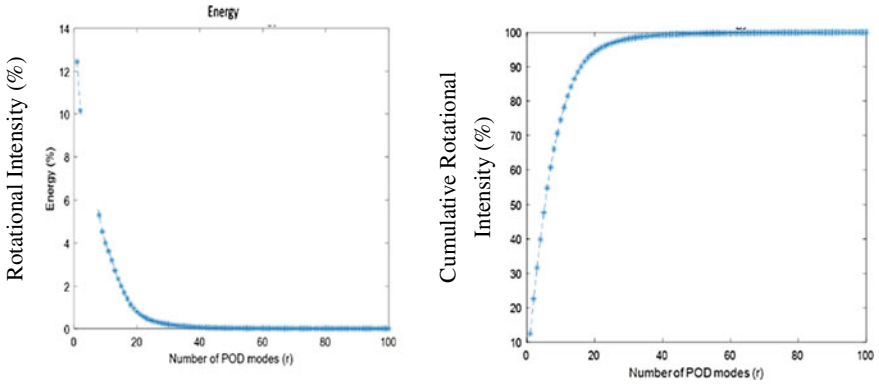

Fig. 6.2 **a** Rotational intensity at various POD modes. **b** Cumulative rotational strength of POD modes

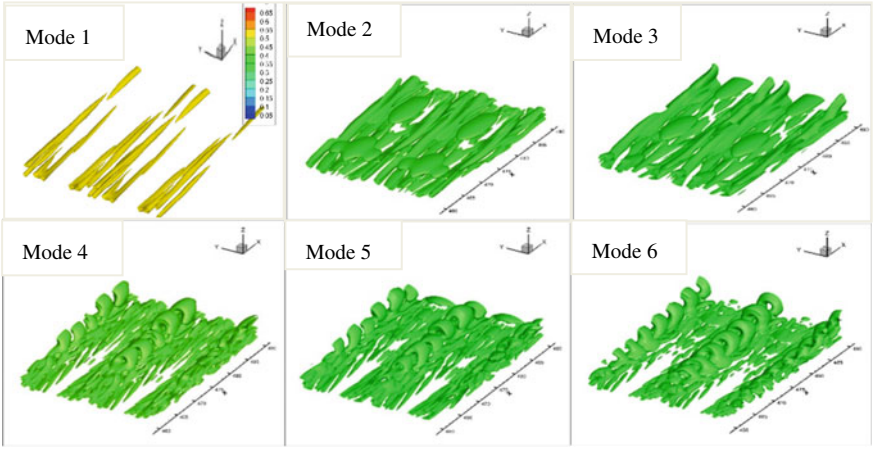

Fig. 6.3 Vortex structures of the first 10 modes with iso-surfaces of $\widetilde{\Omega}_L = 0.52$

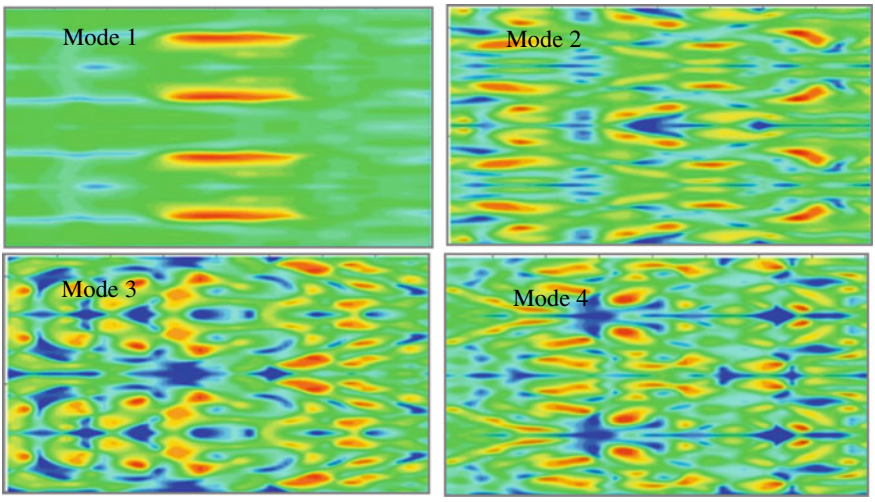

Fig. 6.4 Interior structure of some POD modes by XY-cross section

the fluid rotation. This will reduce the size of the original data, keeping most of the features of data (fluctuating vortex strength) intact. This can be seen in Fig. 6.5, where the first five POD modes model the original fluid flow.

Definition 6.2 The coefficients that we get when the eigenvector matrix Φ_k in Eq. 6.2 are scaled by the singular values of the original matrix are known as POD time coefficients. The POD time coefficients $a_k(t)$ function as a weight factor for each mode.

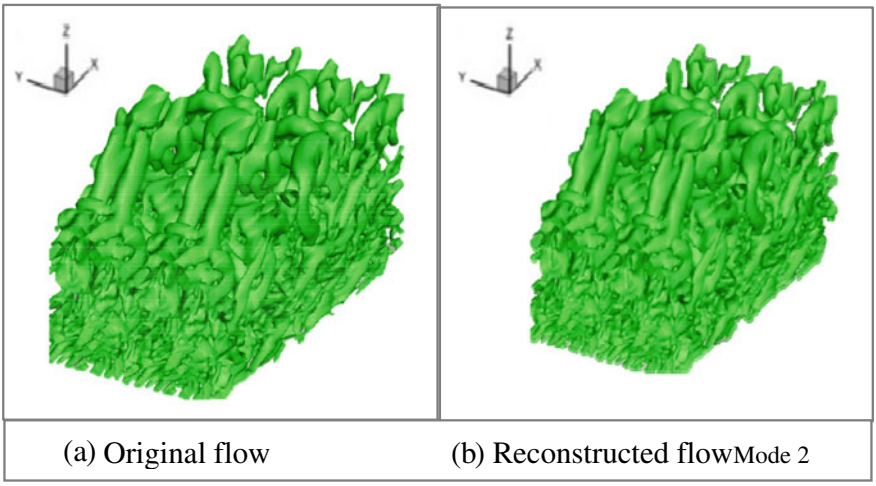

Fig. 6.5 Vortex structures of original and reconstructed flow by first five modes with of $\widetilde{\Omega}_L = 0.52$

The time coefficients are representative of flow dynamics. Each column of matrix Φ_k represents the time evolution of the respective mode. The first column gives the time coefficient of the mean flow (1st mode). Similarly, the second column of the eigenvector matrix Φ_k gives the time coefficient of the second mode, and so on. Then, these modes are scaled by the corresponding singular values. The following graphs show the POD time coefficients of the first five modes. The remaining time coefficients show a similar fluctuating structure, so they are omitted (Fig. 6.6).

These graphs demonstrate the dynamics (fluctuations) of fluid motion. The mean flow has the least fluctuation, while the higher modes have more significant fluctuations. Some similar fluctuations can be seen in the trailing modes.

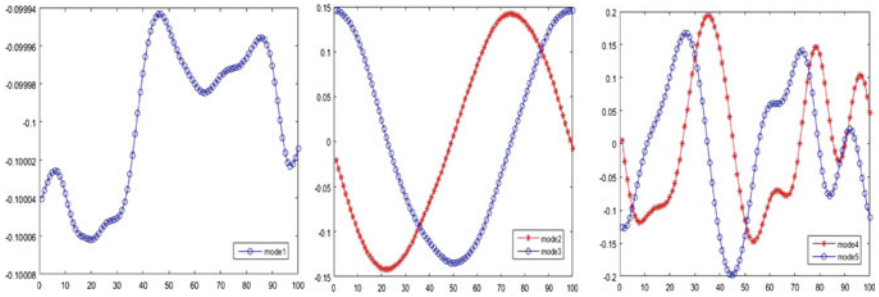

Fig. 6.6 POD time coefficients of mode 1 to mode 5, where the x-axis represents time steps, and the y-axis represents time coefficients

6.5 POD Analysis on Losing Symmetry of Vortex Structure

The vortex structure in the early stage is symmetric. However, it starts to lose the symmetry in the transition stage, and at the late transition stage, the vortex structure is entirely chaotic, making it asymmetric. We have probed the zone where vortex symmetry is being lost and examined the areas from where it starts to lose symmetry. The following figure shows that the top part of the vortex structure is symmetric near X = 470, but the bottom is already antisymmetric at the same time step and position (Fig. 6.7).

From Fig. 6.8a, it can be seen that at X = 470, the vortex structure at the top, middle, and bottom are all symmetric. In Fig. 6.8b the middle part is antisymmetric while the top and bottom are still symmetric. However, in Fig. 6.8c, we can see that the top, middle, and bottom are completely antisymmetric. The index for grid-level along the z-axis for bottom, middle and top are k = 0–1, k = 1–4 and k = 4+ respectively.

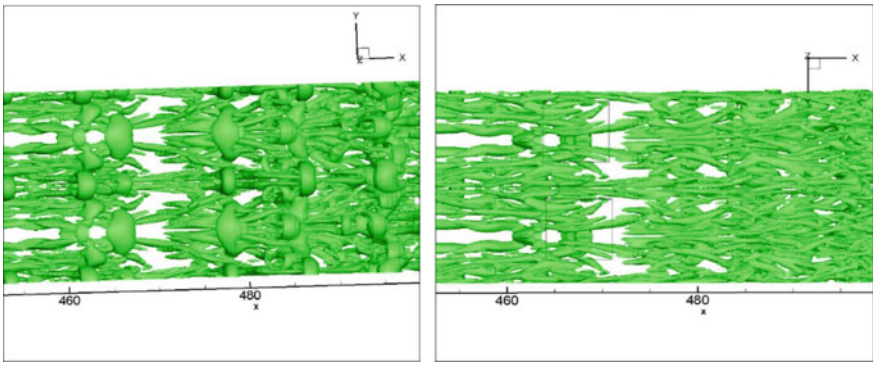

Fig. 6.7 Top and bottom views of the vortex structure at the same position

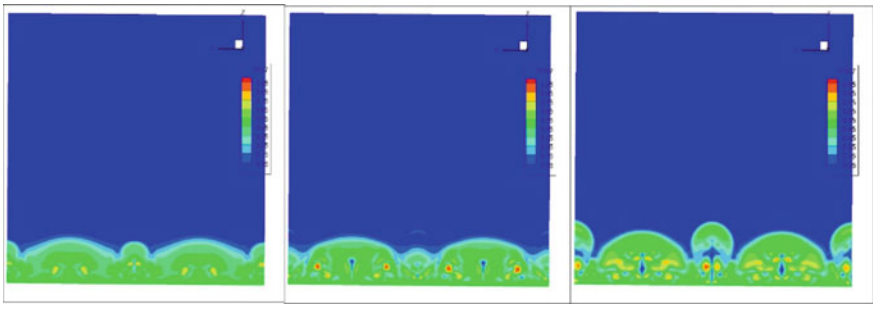

Fig. 6.8 YZ-slice of flow structure at X = 470, X = 475, and X = 480

Definition 6.3 The function $f(x, y, z)$ is symmetric about plane $y = 0$ axis along the spanwise direction in the domain $-\pi \leq y \leq \pi$ if $f(x, -y, z) = f(x, y, z)$ for $\forall x, y, z \epsilon Z^+$.

Definition 6.4 Let $L_{i,j,k}$ be the Liutex magnitude where i, j, k are indexes for grid points along the x, y, and z directions, respectively. Let the domain of grid points be $i \in [i_1, i_2]$, $j \in [2, 128]$, and $k \in [1, 200]$. The YZ plane at y = 0 (i.e. $j = 64$) is the axis of symmetry. $L_{j,k}$ and $L_{128-j,k}$ are the Liutex magnitudes for $j = 2, 3, \ldots, 64$ in the YZ-plane on the left and right of the axis of symmetry, respectively.

Two points, x(:,j, k) and x(:, 128-j, k), at any $i \in [i_1, i_2]$ are symmetric about the plane $y = 0$ at $z = k$ for $k = 1, 2, \ldots, 200$ if $\left|L_{j,k} - L_{130-j,k}\right| < 0.001$; otherwise, these two points are not symmetric about the plane y = 0.

Let $m(d_i)$ and $n(d_i)$ are the number of pairs of points that are symmetric and antisymmetric, respectively. The antisymmetric index is defined by

$$\alpha_i = \left(\frac{n(d_i)}{m(d_i) + n(d_i)}\right). \tag{6.4}$$

For $i \in [i_1, i_2]$, the contour of Liutex magnitude in the YZ-plane is symmetric about the plane $y = 0$ if $\alpha_i < 0.01$. Otherwise, the contour of Liutex magnitude in the YZ-plane is antisymmetric about $y = 0$. So, the vortex structure is symmetric about $y = 0$ if $\alpha_i < 1$, $\forall i \in [i_1, i_2]$. Otherwise, the vortex structure is antisymmetric about $y = 0$.

From the above definition, if $\alpha_i \geq 1$, the vortex structure is antisymmetric. The higher the value of α_i, the more antisymmetric the vortex structure is. If $\alpha_i < 1$, symmetric vortex exists (Figs. 6.9 and 6.10).

The figure is the YZ-slice contour of the reconstruction of the vortex structure by the first five modes at timestep t = 20.00 T, where T is the period of T-S wave.

This figure shows that in reconstructed data, the bottom part has crossed the antisymmetric index threshold (i.e., 0.01) at around X = 468. Then the middle and top part crosses that limit at X = 470 and X = 475, respectively, indicating that the antisymmetric vortex structure starts from the middle, then spreads to the bottom, and then to the top of the boundary layer vortex structure in transitional flow.

6.6 Conclusion

POD can be used to reduce the dimension of the large data, keeping most of the features intact. This will reduce the cost and time of computation. So, this technique has been so effectively applied in the literature. From the POD analysis on losing symmetry of vortex structure in the boundary layer transition, we can conclude the followings:

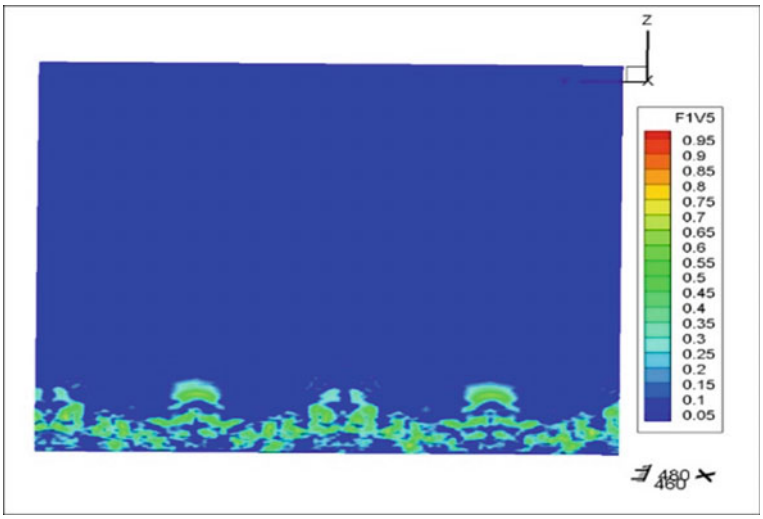

Fig. 6.9 YZ-slice of reconstructed flow by the first five POD modes at X = 470

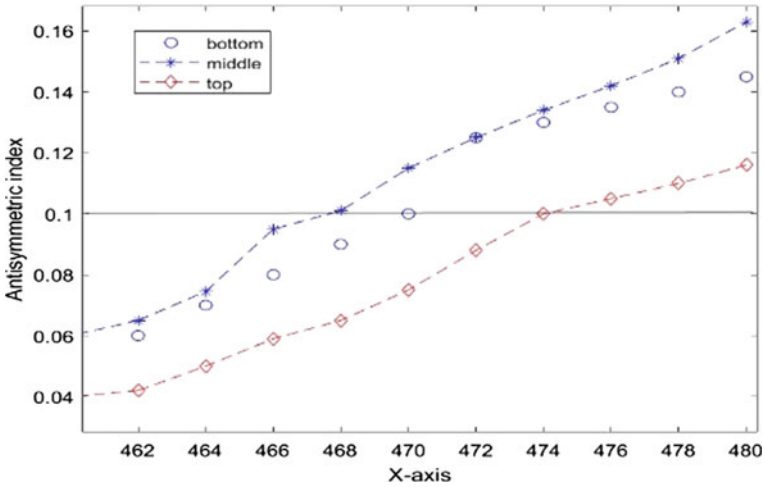

Fig. 6.10 The antisymmetric index of the top, bottom, and middle part of the reconstructed vortex structure by the first five POD modes

1. Mode 1, known as the mean flow, has most of the rotational intensity of the flow. Leading modes have dominant rotational strength, while trailing modes contribute less to fluid rotation.
2. The first three/four modes have streamwise characteristic, but when we take higher modes, the spanwise characteristic of the flow becomes dominant.

3. The antisymmetry of the vortex structure starts from the middle of the boundary layer, and then the antisymmetric structure of the bottom part starts and spreads to the top level. In the late transition stage of the boundary layer, the vortex structure is entirely asymmetric.

References

1. J.L. Lumley, The structure of inhomogeneous turbulent flows. Atmospheric Turbulence and Radio Wave Propagation, pp.166–178 (1967)
2. L. Sirovich, Turbulence and the dynamics of coherent structures. Part I: coherent structures. Q. Appl. Math. **45**(3), 561–571 (1987)
3. S. Charkrit, P. Shrestha, C. Liu, Liutex core line and POD analysis on hairpin vortex formation in natural flow transition. J. Hydrodyn. **32**, 1109–1121 (2020). https://doi.org/10.1007/s42241-020-0079-0
4. P. Shrestha, C. Nottage, Y. Yu et al., Stretching and shearing contamination analysis for Liutex and other vortex identification methods. Adv. Aerodyn. **3**, 8 (2021). https://doi.org/10.1186/s42774-020-00060-9
5. M.S. Chong, A.E. Perry, A general classification of three-dimensional flow fields. Phys. Fluids A **2**(5), 765–777 (1990)
6. J. Jeong, F. Hussain, On the identification of a vortex. J. Fluid Mech. **285**, 69–94 (1995)
7. J.C.R. Hunt, A.A. Wray, P. Moin, Eddies, stream, and convergence zones in turbulent flows. Center for Turbulent Research Report CTR-S88, 193–208 (1988)
8. J. Zhou, R. Adrian, S. Balachandar, T.M. Kendall, Mechanisms for generating coherent packets of hairpin vortices in channel flow. J. Fluid Mech. **387**, 353–396 (1999)
9. C. Liu, Y. Gao, X. Dong, Y. Wang, J. Liu, Y. Zhang, X. Cai, N. Gui, Third generation of vortex identification methods: omega and Liutex/Rortex based systems. J. Hydrodyn. **31**(2), 205–223 (2019)
10. C. Liu, Y. Gao, S. Tian, X. Dong, Rortex-a new vortex vector definition and vorticity tensor and vector decompositions. Phys. Fluids **30**, 035103 (2018)
11. Y. Gao, C. Liu, Rortex and comparison with eigenvalue-based identification criteria. Phys. Fluid **30**, 085107 (2018)
12. Y. Gao, J. Liu, Y. Yu, C. Liu, A Liutex based definition and identification of vortex core center lines. J. Hydrodyn. **31**(3) (2019)
13. O. Alvarez, Y. Yu, P. Shrestha, D. Almutairi, C. Liu, Visualizing liutex core using liutex lines and tubes, in C. Liu, Y. Wang (eds.), *Liutex and Third Generation of Vortex Definition and Identification*. Springer, Cham (2021). https://doi.org/10.1007/978-3-030-70217-5_10
14. Y. Yu, P. Shrestha, O. Alvarez, C. Nottage, C. Liu, Investigation of correlation between vorticity, Q, λci, λ2, Δ and Liutex. Comput. Fluids **225**, 104977 (2021), ISSN 0045-7930.https://doi.org/10.1016/j.compfluid.2021.104977
15. Y. Yu, P. Shrestha, O. Alvarez, C. Nottage, C. Liu. Correlation analysis among vorticity, Q method and Liutex. J. Hydrodyn. **32** (2020).https://doi.org/10.1007/s42241-020-0069-2
16. P. Shrestha, A. Bhattarai, C. Liu, Application of liutex and some second-generation vortex identification methods to direct numerical simulation data of a transitional boundary layer, in: C. Liu, Y. Wang (eds.), *Liutex and Third Generation of Vortex Definition and Identification*. Springer, Cham (2021). https://doi.org/10.1007/978-3-030-70217-5_19
17. Y. Yu, P. Shrestha, O. Alvarez, C. Nottage, C. Liu, Incorrectness of the second-generation vortex identification method and introduction to liutex, in C. Liu , Y. Wang (eds.), *Liutex and Third Generation of Vortex Definition and Identification*. Springer, Cham (2021). https://doi.org/10.1007/978-3-030-70217-5_2

18. C. Nottage, Y. Yu, P. Shrestha, C. Liu, Dimensional and theoretical analysis of second-generation vortex identification methods, iIn C. Liu, Y. Wang (eds.), *Liutex and Third Generation of Vortex Definition and Identification*. Springer, Cham (2021). https://doi.org/10.1007/978-3-030-70217-5_3
19. H. Gunes, Proper orthogonal decomposition reconstruction of a transitional boundary layer with and without control. Phys. Fluids **16** (2004), Article ID 2763
20. Y. Yang, S. Tian, C. Liu, POD Analyses on Vortex Structure in Late-stage Transition," AIAA paper 2018–0821, January 2018
21. X. Dong, X. Cai, Y. Dong, C. Liu, POD analysis on vortical structures in MVG wake by Liutex core line identification. J. Hydrodyn. (2020)